Supplementary information

4-*tert*-butylpyridine coordination to alkylammoniums in perovskites

Naoyuki Nishimura, Yoyo Hinuma, Hiroyuki Kanda, Takurou N. Murakami*

National Institute of Advanced Industrial Science and Technology (AIST), 1-1-1 Higashi, Tsukuba, Ibaraki 305-8565, Japan.

*Corresponding Author

Naoyuki Nishimura, E-mail: naoyuki-nishimura@aist.go.jp

1. Molecular structures

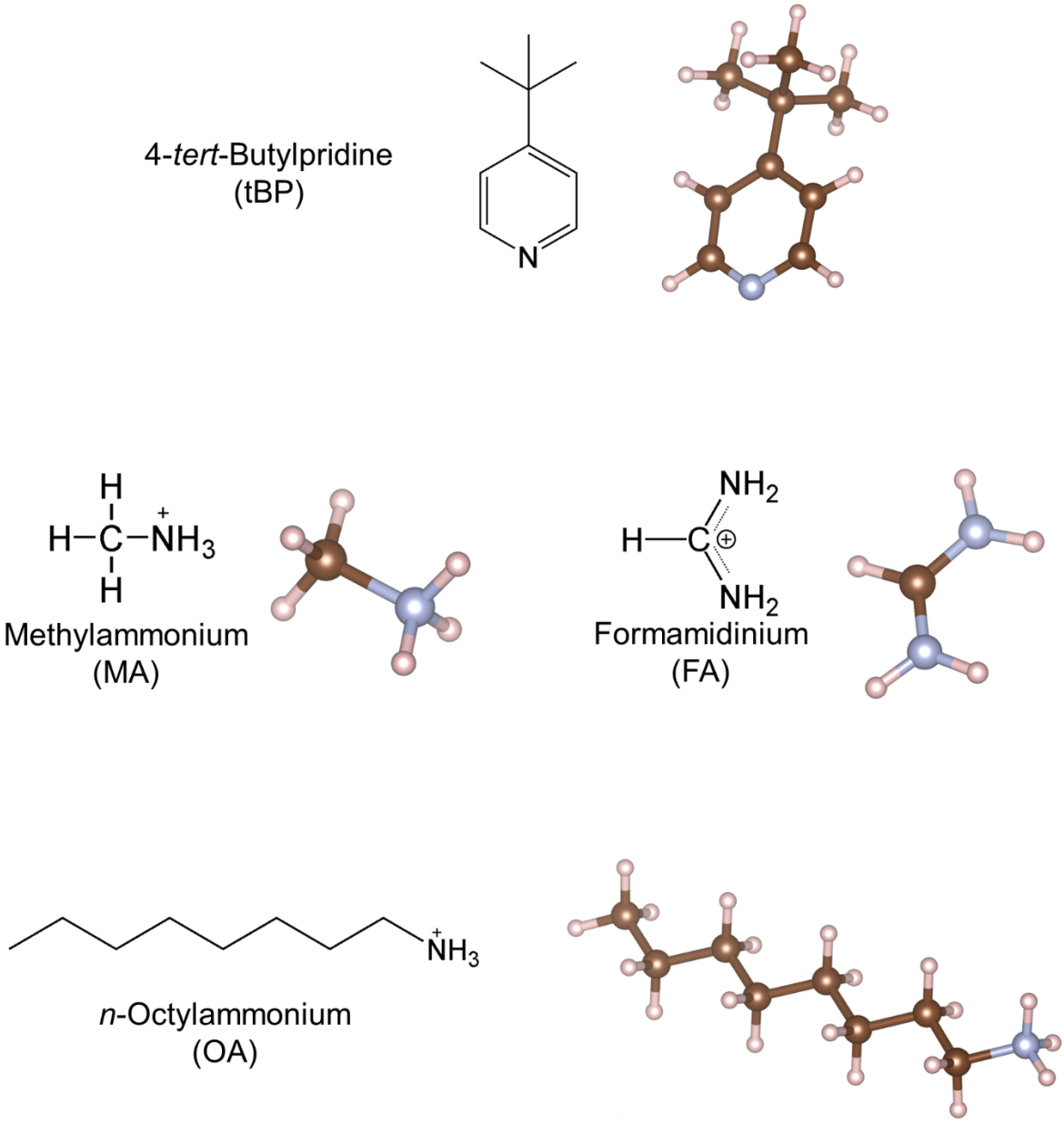

Fig. S1 Molecular structures of 4-tert-butylpridine (tBP), methylammonium (MA), formamidinium (FA), and *n*-octylammonium (OA)

2. Spontaneous perovskite passivation by OA-TFSI

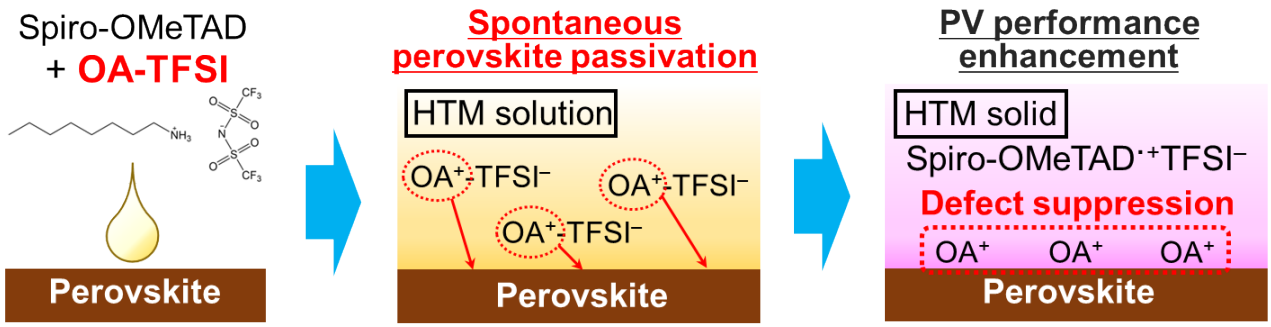

Fig. S2 Schematic of spontaneous perovskite passivation during HTM deposition using an OA-TFSI-containing Spiro-OMeTAD solution; during deposition, OA cations spontaneously migrate to the perovskite surface and effectively suppress surface defects, enhancing the photovoltaic (PV) performance.

3. tBP coordination to alkylammoniums

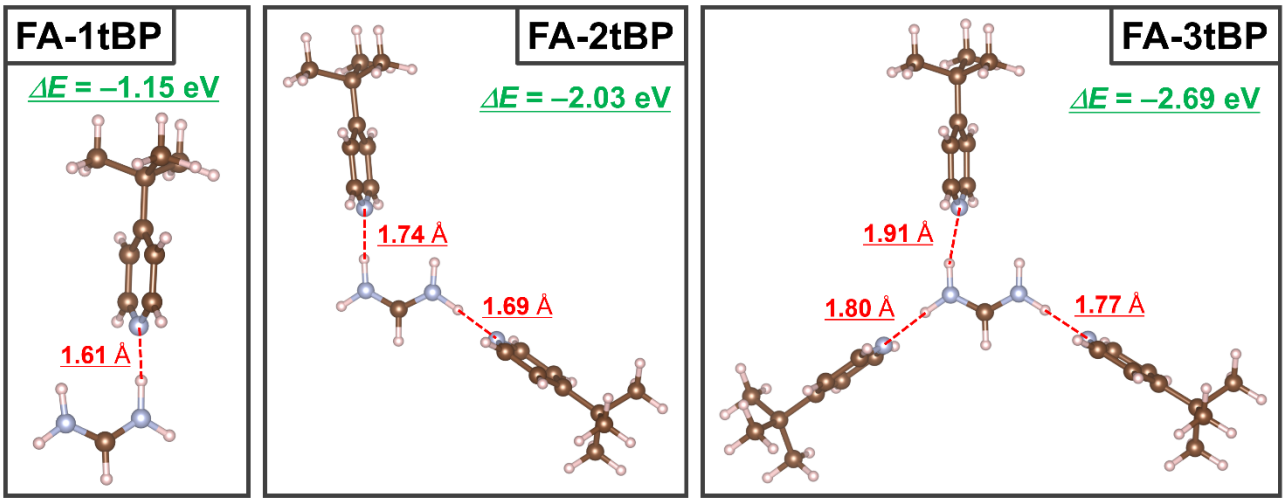

Fig. S3 tBP coordination to FA with 1, 2, and 3 tBP molecules

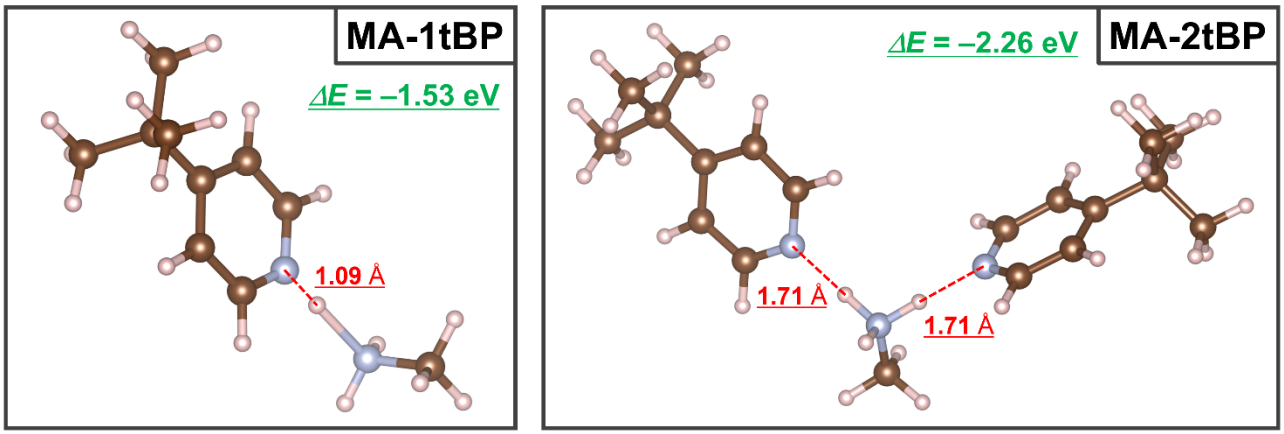

Fig. S4 tBP coordination to MA with 1 and 2 tBP molecules

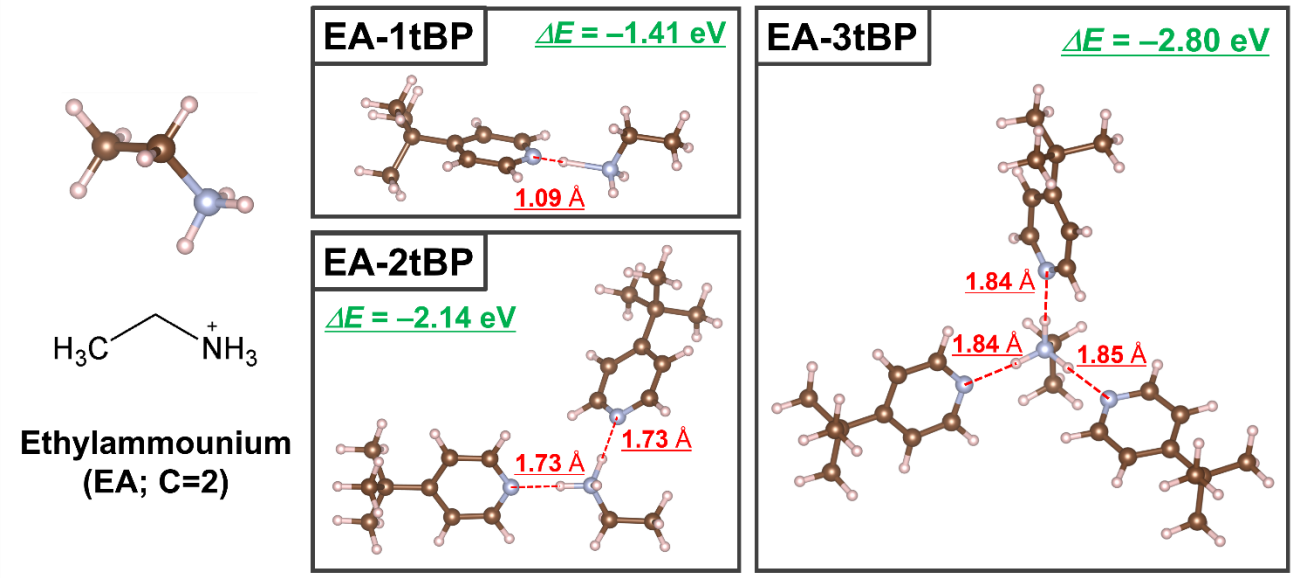

Fig. S5 tBP coordination to ethylammonium (EA) with 1, 2, and 3 tBP molecules

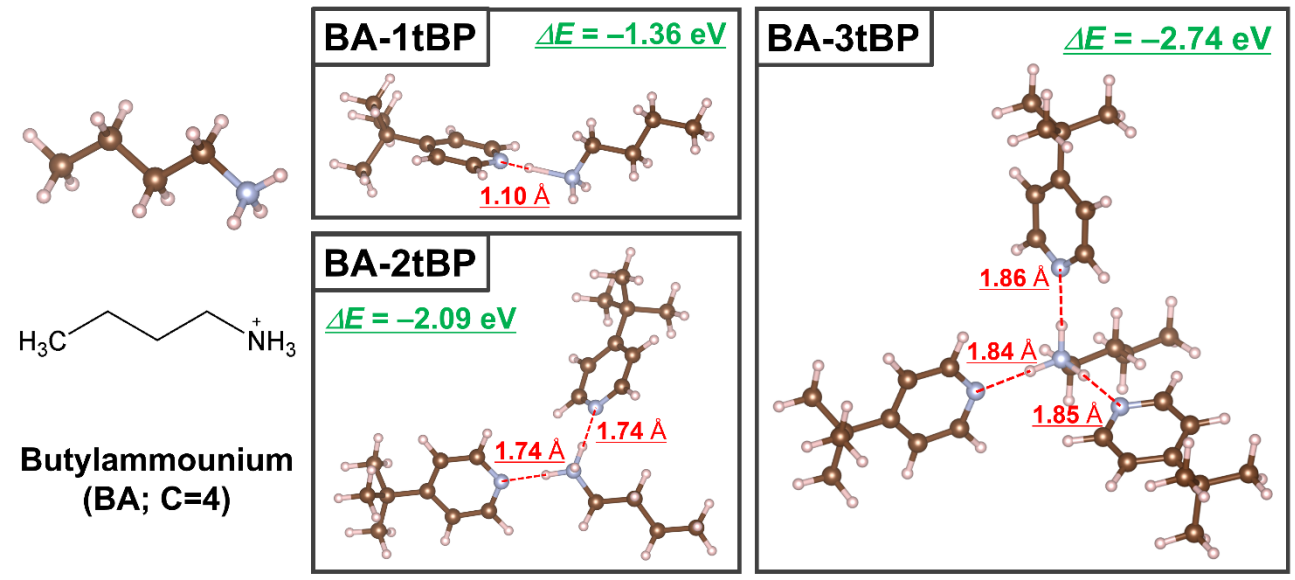

Fig. S6 tBP coordination to butylammonium (BA) with 1, 2, and 3 tBP molecules

Table S1. Summary of the net energy of tBP coordination

Molecule	Coordination energy via strong hydrogen bonding (ΔE; eV)			
	tBP×1	tBP×2	tBP×3	tBP×4
FA	-1.15	-2.03	-2.69	-3.15
MA	-1.53	-2.26	-2.96	
EA	-1.41	-2.14	-2.80	
BA	-1.36	-2.09	-2.74	
OA	-1.25	-2.07	-2.72	

4. Spontaneous perovskite passivation mechanism with OA-3tBP

Table S2. Energy changes associated with OA-*x*tBP adsorption on an $FAPbI_3$ surface

	Free	OA-3tBP adsorption	Intermediate	OA-2tBP adsorption	OA-1tBP adsorption	Sole OA adsorption
Net system	0	–1.37	–1.05	–0.9	–0.47	–0.23
tBP dissociation	—	—	—	0.68	1.40	2.90
OA-focused	0	–1.37	–1.05	–1.58	–1.87	–3.13

The OA-focused absorption energies (Fig. 3) were calculated using the following equation:

$$E_{\text{OA-focus}} = E_{\text{net}} - E_{\text{tBPdiss}} \qquad \text{(S1)}$$

where $E_{\text{OA-focus}}$, E_{net}, and E_{tBPdiss} denote the OA-focused absorption energy, net energy of the system, and energy for tBP dissociation from OA in the calculation slab, respectively. The dissociation energy of OA–tBP was calculated by moving the tBP molecules 15 Å away from the slab, one at a time. When multiple tBP molecules were close to each other in a vacuum after this procedure, the tBP molecules were moved by up to a few Å to separate them.

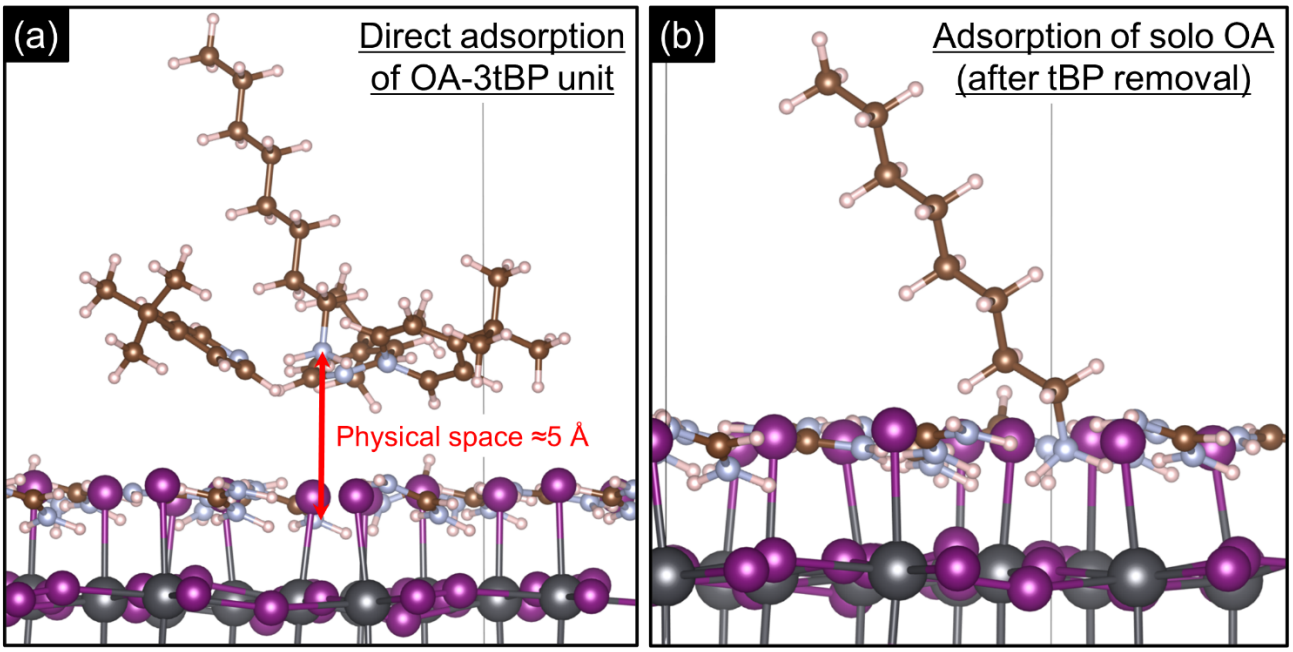

Fig. S7 Enlarged illustration of OA (unit) adsorption on a perovskite surface shown in Fig. 3: (a) direct adsorption of OA-3tBP unit forming substantial physical space between OA and the perovskite surface, and (b) adsorption of solo OA after the removal of all tBP molecules

5. Cross-sectional SEM images of perovskite solar cells (PSCs)

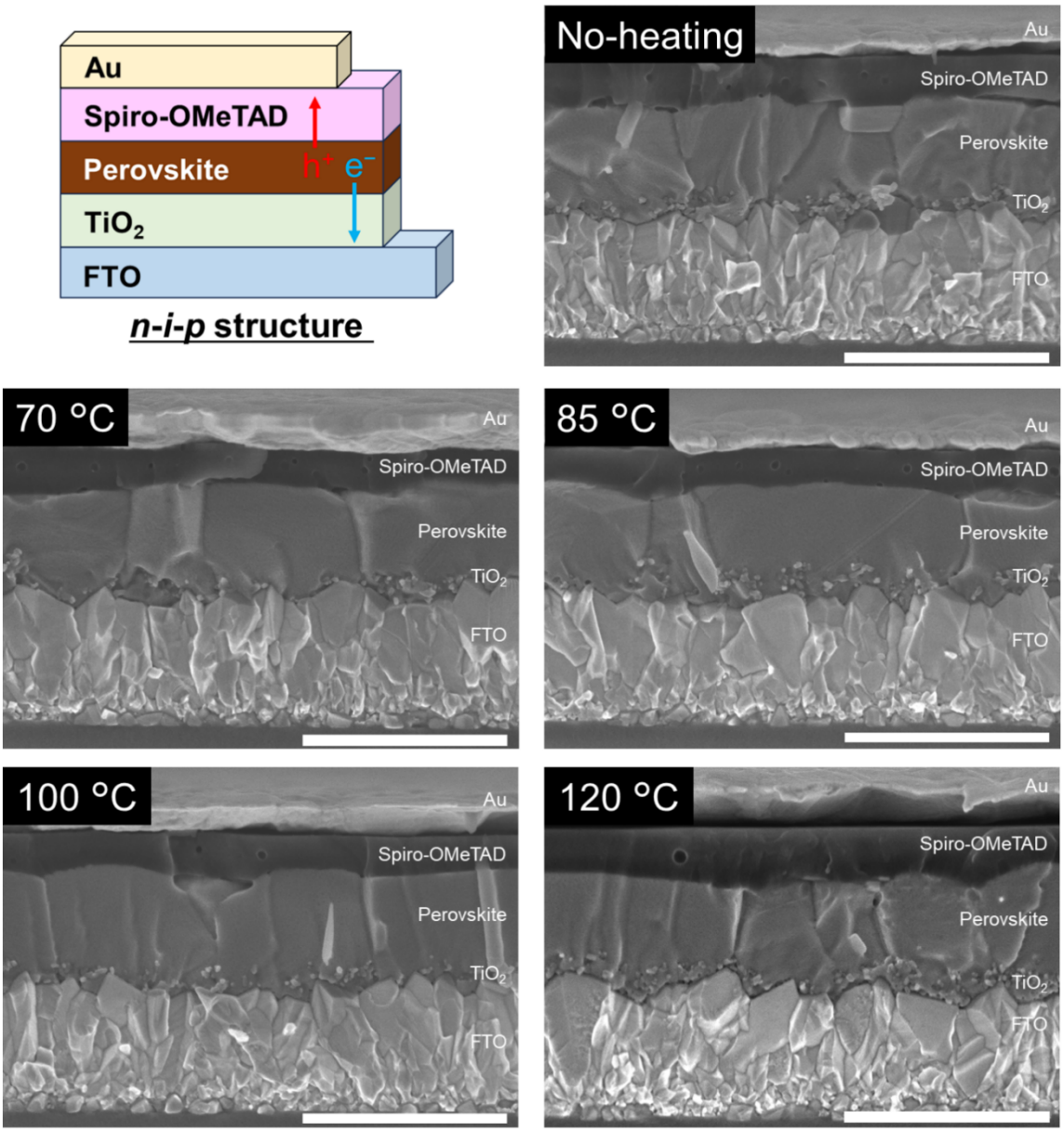

Fig. S8 Cross-sectional images of the PSCs obtained using OA-TFSI HTM additives with and without post-heating treatment at various temperatures

6. Compositional depth analysis

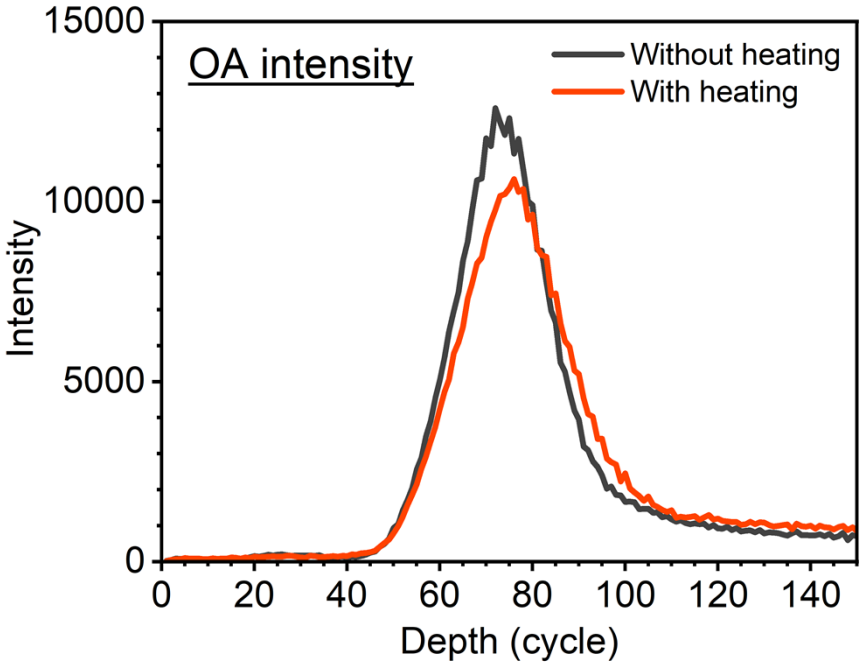

Fig. S9 Comparison of OA intensities of ToF-SIMS for the samples with and without post-heating (Fig. 4a and 4b) with a linear scale on the *y*-axis.

7. PV performance

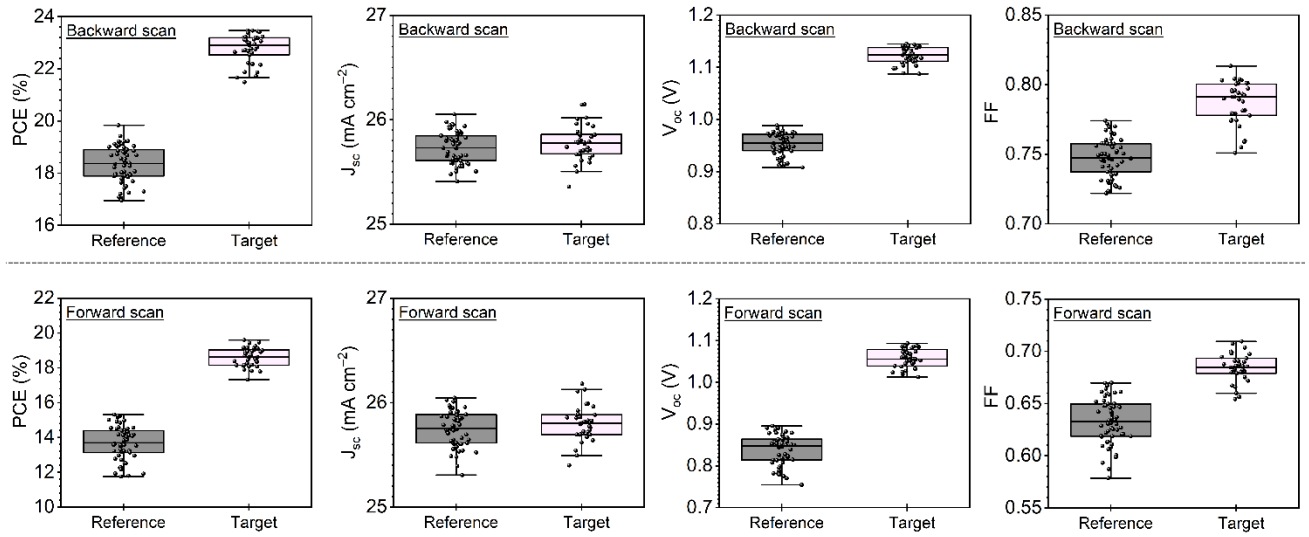

Fig. S10 PV parameter distribution of PSCs with a conventional set of dopants (Li-TFSI + tBP + FK209: reference) and OA-TFSI combining optimal post-heating at 85 °C (target)

Table S3 PV parameters of PSCs with a conventional set of dopants (reference) and OA-TFSI combining optimal post-heating at 85 °C (target)

Sample	Scan	Average / Best	J_{sc} (mA/cm^2)	V_{oc} (V)	FF	PCE (%)
Reference	Backward	Best	25.9	0.99	0.77	19.8
		Average	25.7 ± 0.2	0.95 ± 0.02	0.75 ± 0.01	18.3 ± 0.7
	Forward	Best	25.9	0.88	0.67	15.2
		Average	25.7 ± 0.2	0.84 ± 0.04	0.63 ± 0.02	13.7 ± 1
OA-TFSI 85 °C	Backward	Best	25.8	1.14	0.80	23.5
		Average	25.8 ± 0.2	1.12 ± 0.02	0.79 ± 0.02	22.8 ± 0.5
	Forward	Best	25.8	1.09	0.68	19.1
		Average	25.8 ± 0.2	1.06 ± 0.02	0.68 ± 0.01	18.6 ± 0.5

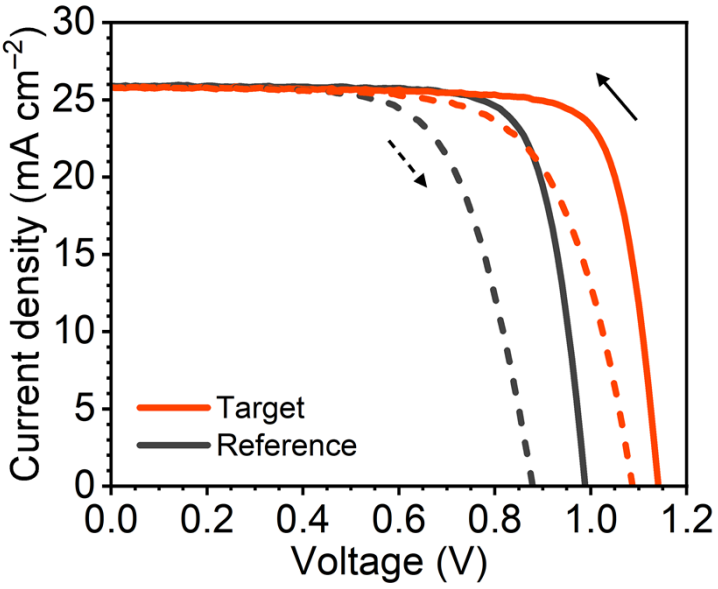

Fig. S11 *J–V* curves of the best-performing PSCs with a conventional set of dopants (reference) and OA-TFSI combining optimal post-heating at 85 °C (target)

Fig. S10, S11, and Table S3 show the PV performance of the PSCs with the conventional set of dopants (Li-TFSI, tBP, and FK209) or OA-TFSI subjected to optimal post-heating at 85 °C. PSCs with OA-TFSI exhibited better PV performance, confirming its spontaneous perovskite passivation effects. For instance, the average power conversion efficiency (PCE) of PSCs with OA-TFSI was higher (22.8 ± 0.5 % (best: 23.5 %)) than those of PSCs with the conventional set of dopants (18.3 ± 0.7 % (best: 19.8 %)) in backward scan, primarily attributed to an increase in the open-circuit voltage (V_{oc}) from 0.95 ± 0.02 V (best: 0.99 V) to 1.12 ± 0.02 V (best: 1.14 V).

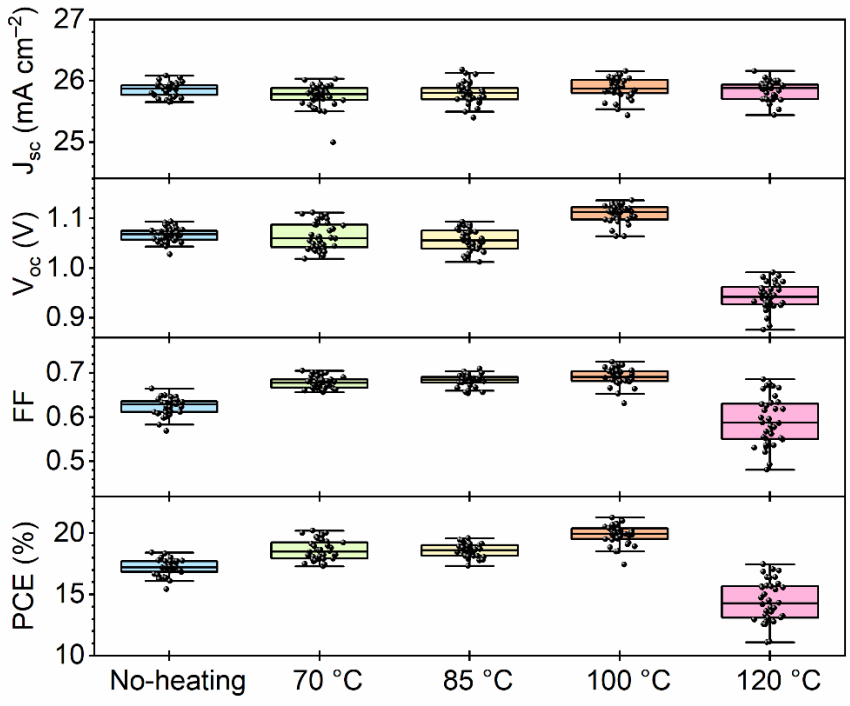

Fig. S12 PV parameter distributions of PSCs with OA-TFSI and post-heating treatments at various temperatures in forward scan (backward scan: Fig. 5)

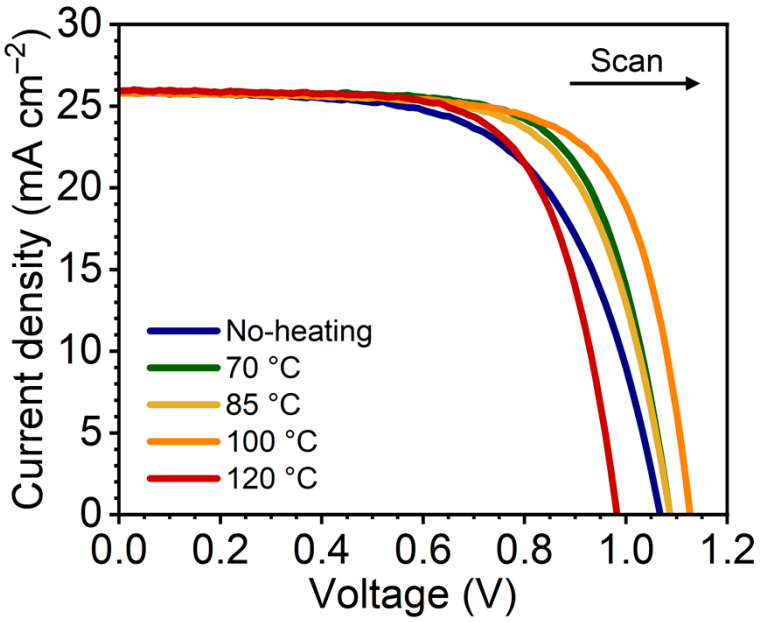

Fig. S13 *J–V* curves of PSCs with OA-TFSI and post-heating treatments at various temperatures in forward scan (backward scan: Fig. 6a)

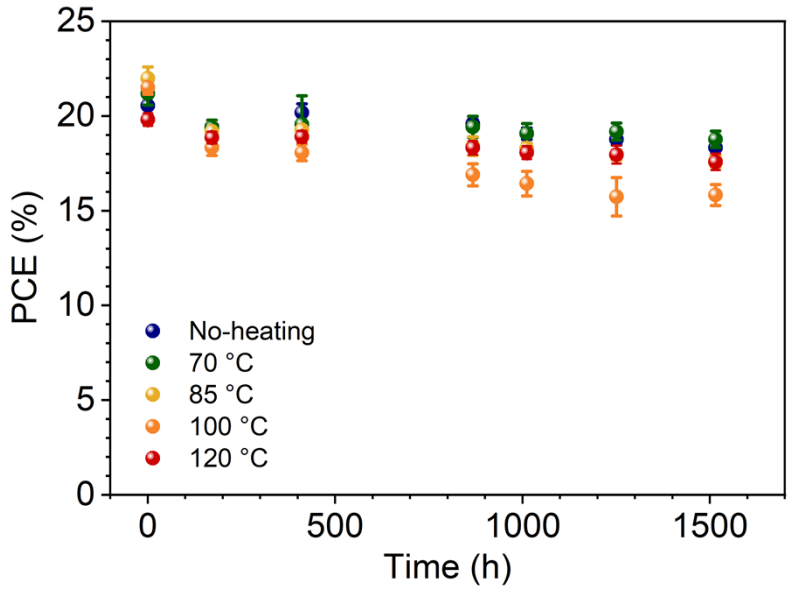

Fig. S14 Long-term stability of PSCs in the presence of humidity (50% relative humidity at 30 °C) without encapsulation

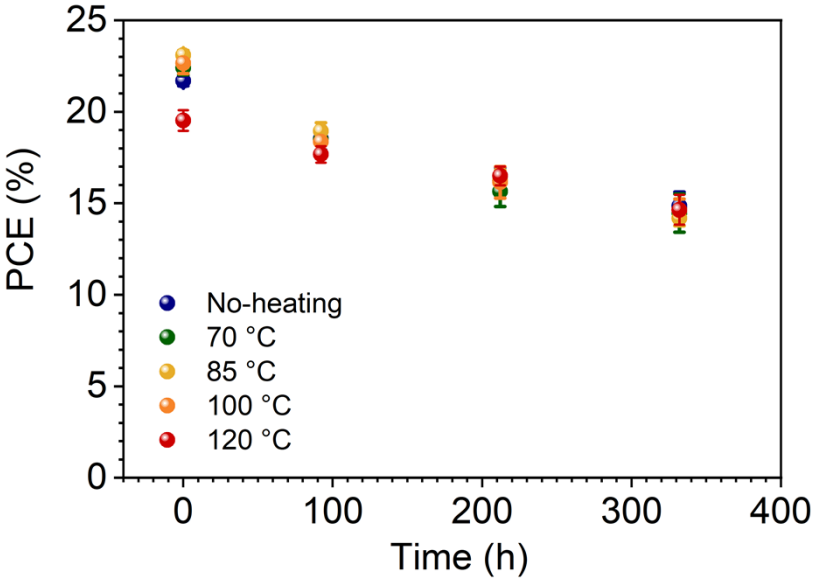

Fig. S15 Long-term stability of PSCs at an elevated temperature of 65 °C in a nitrogen atmosphere without encapsulation

Table S4 Series resistances (*Rs*) of PSCs and PL lifetimes (τ) of spiro-OMeTAD/perovskite bilayer samples prepared using OA-TFSI + tBP with post-heating at various temperatures, corresponding to Fig. 7

Post-heating temperature	Series resistance R_s (Ω)	PL lifetime τ (ns)
No-heating	29 ± 4	25.0 ± 0.9
70 °C	22 ± 2	19.5 ± 0.3
85 °C	18 ± 1	8.22 ± 0.15
100 °C	19 ± 2	3.88 ± 0.23
120 °C	21 ± 3	2.93 ± 0.07